THE JOURNAL OF PHYSICAL CHEMISTRY C
A JOURNAL OF THE AMERICAN CHEMICAL SOCIETY

pubs.acs.org/JPCC

Article

Thermally Stable Concentrated Solutions of Molecular Hydrogen in Bulk Lithium Silicate Glass

V. S. Efimchenko,* M. A. Korotkova, K. P. Meletov, and S. Buchner

Cite This: J. Phys. Chem. C 2023, 127, 13538−13546

Read Online

ACCESS | Metrics & More | Article Recommendations

ABSTRACT: This paper is aimed at studying the effect of Li cations on the thermal stability of concentrated solid solutions of molecular hydrogen in the $Li_2O{\cdot}6SiO_2$-$0.39H_2$ and $Li_2O{\cdot}6SiO_2$-$0.25H_2$ compounds synthesized at pressures of 7.5 and 6.6 GPa and a temperature of 280 °C. The decomposition of the solutions was examined by Raman scattering under isothermal annealing at 21−70 °C and by hot hydrogen desorption into a pre-evacuated volume at 0−97 °C. The activation energies E_a = (0.419 ± 0.019) and (0.411 ± 0.06) eV/H_2 of hydrogen desorption from the near-surface layer of the samples with $0.39H_2$ and $0.25H_2$, respectively, determined by Raman spectroscopy were higher than E_a = (0.16 ± 0.02) eV/H_2 previously determined for hydrogenated pure silica glass. This suggests the occurrence of a "Kubas" or similar interaction between the lithium cations and hydrogen molecules. The interaction leads to a large decay time constant of τ = 3220 s at room temperature compared to τ = 3 s for the hydrogen solutions in pure silica glass. The hot desorption showed that the diffusion activation energy was higher than 0.51 eV and also had a great impact on the stability of the hydrogen solutions in bulk lithium silicate glass, which additionally increased the decay time constants several times.

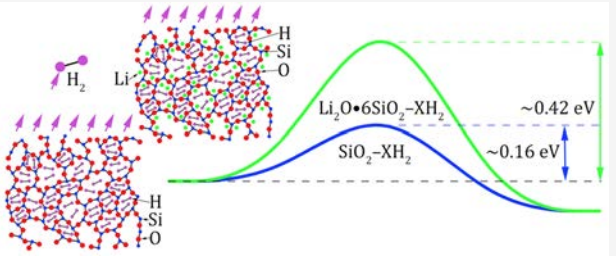

INTRODUCTION

It is known that materials for hydrogen storage should have a great hydrogen content of more than 6 wt % and consist of abundant and inexpensive elements to be used in practice.[1] However, it is equally important for this prospective material to decompose at temperatures of −10 ÷ 100 °C and at pressures close to normal ones. Most chemical and metal hydrides decompose at temperatures close to or exceeding 100 °C. For example, the most prominent hydrides AlH_3 and MgH_3 decompose at temperatures of 100 and 300 °C, respectively.[2,3] To decrease decomposition temperatures and improve hydrogen adsorption/desorption rates, metal and chemical hydrides are usually milled and/or doped with elements that reduce the energy of bonds between hydrogen and host atoms.[4,5]

Nevertheless, the hydrides that contain hydrogen in the molecular form H_2 have better absorption and desorption kinetics even as compared with doped and milled chemical and metal hydrides.[6−8] This advantage is due to weak van der Waals bonds with the energy of interaction between molecular hydrogen and the atoms of host elements of E < 0.1 eV/H_2.[9−12] However, this low interaction energy leads to the desorption temperature often being much less than 77 K or to higher pressures necessary to keep the hydride. According to many theoretical and some experimental data, the atoms of transition elements in the low-valence state[13−16] and alkaline elements[17−19] as well as defects[20] incorporated in the lattice of nanoporous organic polymers and carbon materials, metal−organic, covalent organic, and porous aromatic frameworks can increase the interaction energy of a hydrogen molecule with the surrounding material by several times due to the Kubas or similar interaction. For example, the "Kubas" forces lead to an energy of interaction between the H_2 molecules and host atoms of about 0.1−0.8 eV/H_2 and can increase the desorption temperature to the desired values of T = 0−100 °C. However, all previous studies were devoted to determining the enthalpy of formation of the solid hydrogen solutions and the maximum hydrogen capacity of the materials under study. The decay time constants and hydrogen desorption activation energies, which are the key parameters for the prediction of thermal stability of molecular solutions under normal conditions, were not determined.

Earlier, our study showed that hydrogen was dissolved in the powder of amorphous silica in the molecular form and hydrogen solubility increased to the molar ratio H_2/SiO_2 = 0.53 at P = 7.5 GPa and T = 250 °C.[21] At normal pressure, this solid solution started to decompose at T = −187 °C and released all dissolved hydrogen at T = 25 °C. Recently studied

Received: April 21, 2023
Revised: June 25, 2023
Published: July 10, 2023

solid solutions of molecular hydrogen in amorphous magnesium silicates demonstrated a similar desorption temperature.[22] However, the temperature range of hydrogen desorption increased with an increase in the concentration of magnesium cations. For example, the $Mg_{0.88}SiO_{2.88} \div 0.26H_2$ solid solution lost about 0.09 mol of H_2 in the temperature range of −187 ÷ 25 °C, whereas other 0.17 mol of dissolved hydrogen escaped from the sample at T = 25 ÷ 400 °C. We concluded that this effect was due to the more close-packed structure of $Mg_{0.88}SiO_{2.88}$ in comparison with the silica glass. The magnesium cations, which penetrated the silicate structure, created efficient "barriers" for hydrogen diffusion and thus extended the temperature range of the desorption. However, the desorption still started at T = −187 °C due to the large surface area of the powder sample.

The hydrogenation of the bulk sample of silica glass allowed us to increase H_2 content to X = 0.7 at P = 7.5 GPa and T = 400 °C, obtain detailed Raman spectra of this solution, and shift desorption temperature by ∼100 °C from −187 °C that was observed earlier for powder samples.[23,24] However, despite a strong decrease in the sample surface area, the main part of dissolved hydrogen (0.6 mol of H_2) escaped from the silica glass during heating to room temperature. Considering the above data on the decomposition of solid solutions in the magnesium silicates and the bulk silica glass, we supposed that it would be possible to create a thermally stable at normal pressure solid solution of molecular hydrogen in the bulk silicate glass, which contained some amounts of cations. Unfortunately, the synthesis of the bulk glass with compositions up to $Mg_{0.88}SiO_{2.88}$ in the MgO-SiO_2 system requires temperatures that exceed the range of T = 1543−2020 °C.[25] Such high temperatures do not allow for the use of most furnaces for glass synthesis. Moreover, in the MgO-SiO_2 system, the glass forming ability strongly depends on the concentrations of magnesium cations and even requires a containerless quenching technology for the samples with high Mg concentrations.[26] Thus, it is better to use oxides that contain cations with dimensions similar to those in MgO but have a lower liquidus temperature. It is also important that the hydrogen dissolved in this silicate glass has the molecular form and does not enter into chemical reactions with the silicate network, as we observed recently for the Fe_2SiO_4−H_2 system.[27,28]

Among all oxides of alkaline and alkaline-earth elements, lithium oxide has three important features. First, the ionic radius of a lithium cation in this oxide r = 7.6 Å is close to the radius r = 7.2 Å for a magnesium cation. Second, the temperature of the liquidus line in the Li_2O-SiO_2 system decreases from 1770 °C for pure SiO_2 to 1028 °C for the Li_2O-$2SiO_2$ composition, which allows one to produce bulk silicate glass at relatively lower temperatures.[29] Third, according to the Ellingham diagram, lithium oxide is one of the most stable compounds in the reduced atmosphere, which allowed one to expect the absence of chemical bonds between hydrogen and the silicate network.[30] Thus, lithium is the most convenient dopant for studying the effect of alkaline or alkaline-earth elements on such parameters of the decomposition kinetics of molecular solutions as decay time constants and activation energy.

In this Article, we report on the results of the hydrogenation of lithium silicate glasses and the decomposition kinetics of the hydrogenated samples. The initial glass samples with Li_2O-$6SiO_2$ composition were loaded with hydrogen at P = 6.6 and 7.5 GPa and T = 280−300 °C. The hydrogenated samples were quenched from these temperatures to the N_2 boiling temperature and were kept in a liquid nitrogen storage Dewar. They were warmed above this temperature when the hydrogen content and thermal stability were studied by hot extraction in vacuum. The hydrogen state in the hydrogenated samples and the kinetics of hydrogen desorption were studied by Raman spectroscopy at ambient pressure in the temperature range of −186−60 °C.

EXPERIMENTAL METHODS

The initial samples of lithium silicate glasses with $Li_2O{\cdot}6SiO_2$ (LS6) compositions were synthesized at the Federal University of Rio Grande do Sul, Brazil, using standard reagent grade Li_2CO_3 (Aldrich Chem. Co. ≥99%) and ground quartz SiO_2 (Aldrich Chemical Co. ≥99.9%). A glass batch was melted in a Pt crucible at 1550 °C for 2 h in an electric furnace, and the melt was poured on a steel plate at room temperature. The hydrogenation of a few samples was carried out in a toroid-type high-pressure apparatus[31] with NH_3BH_3[32] as an internal hydrogen source. The high-pressure cell was made of Teflon or copper; a Pd foil separated the glass samples from the hydrogen source. To release hydrogen, NH_3BH_3 was decomposed at P = 1.5 GPa by heating to T = 250 °C. After that, the pressure and temperature were changed to P = 6.7 GPa and T = 300 °C with a time exposure of 18 h or to P = 7.5 GPa and T = 280 °C with a time exposure of 45 min.

After exposure, the hydrogenated samples were cooled to room temperature and then quenched to −196 °C to prevent hydrogen losses during pressure release. The total molar ratio $X = H_2$/f.u. of the samples was determined with an accuracy of 3% by extraction into the pre-evacuated volume under continuous heating from −196 to 600 °C.[33] The desorption kinetics of the hydrogenated samples into the pre-evacuated volume was studied at fixed temperatures in the range of 0−97 °C by recording the time dependencies of pressure in the pre-evacuated volume.

To determine the hydrogen state (a molecule or an atom) and study the phonon spectrum, the hydrogenated samples were placed in a liquid nitrogen vessel and then studied by Raman spectroscopy at T = −186 °C. The Raman spectra were recorded in backscattering geometry using a micro-Raman setup composed of an Acton SpectraPro-2500i spectrograph and a Pixis2K CCD. The 532 nm line of a single-mode yttrium aluminum garnet (YAG) continuous wave (CW) diode-pumped laser was focused on the sample by an Olympus BX51 microscope using a 50× objective. The spatial resolution was ∼1.5 μm, while the spectral resolution was 2.3 (4.1) cm^{-1} in the spectral region of 536 (685) nm. The laser line was suppressed by an edge filter with OD = 6 and bandwidth of ∼100 cm^{-1}, while the beam intensity before the sample was ∼5 mW. The Raman spectra were recorded at low temperature using an in-house-constructed liquid nitrogen cryostat with cold loading of samples without intermediate warming. The cryostat was equipped with a temperature controller and a resistive heater that provided temperature control in the range between −170 and +70 °C with an accuracy of ±0.4 °C.[34] The regularities of hydrogen desorption at different temperatures were also studied *in situ* from a time-dependent change in the Raman spectra of hydrogenated lithium silicate glasses in the isothermal regime at atmospheric pressure.

https://doi.org/10.1021/acs.jpcc.3c02644
J. Phys. Chem. C 2023, 127, 13538−13546

RESULTS

The hydrogen content of the LS6 samples hydrogenated at P = 6.7 GPa and T = 300 °C was determined by hot extraction; it corresponded to the molar ratios H_2/f.u. = 0.22−0.26 (22−26 mol %). The samples synthesized at the higher pressure P 7.5 GPa and T 280 °C contained 0.39 mol of H_2 per mole of silicate (39 mol %). Figure 1 depicts the thermal desorption

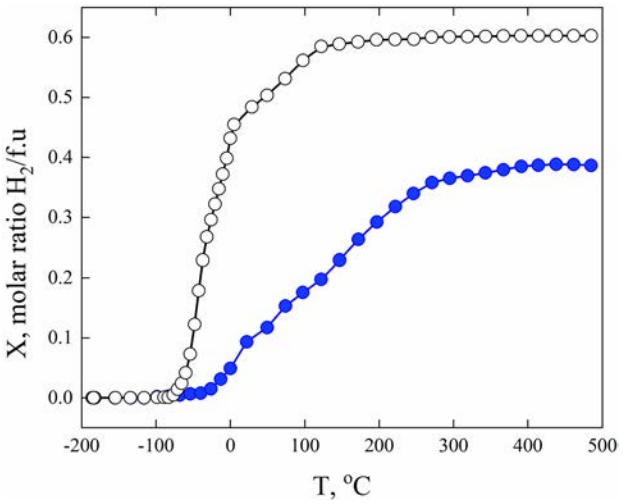

Figure 1. Thermal desorption curve of the SiO_2-0.6H_2 (open black circles)[24] and $Li_2O{\cdot}6SiO_2$-0.39H_2 (filled blue circles) samples.

curves of the sample containing 0.39 mol of H_2 in comparison with the earlier obtained desorption curve of the hydrogenated pure silica glass.[24] The hydrogenated lithium silicate glass started evolving hydrogen at a temperature near −50 °C. The hydrogen was released from this sample in a wide temperature range of −50 ÷ 550 °C, but only 20−30% of the dissolved hydrogen was released at temperatures below 25 °C. In contrast, the SiO_2−H_2 samples of the hydrogenated pure silicate glass released 70% of the dissolved hydrogen at temperatures significantly below 0 °C.

The wide range of hydrogen desorption temperatures that includes T = 100−500 °C usually means the possible existence of hydrogen in the form of an anion. To study the state of dissolved hydrogen, we measured the Raman spectra of the hydrogenated LS6 samples containing 0.39 or 0.26 mol·H_2/f.u. at normal pressure and near liquid nitrogen temperature. Figure 2 depicts the Raman spectra of the hydrogenated LS6 samples with 0.39 mol of hydrogen and pure silica glass at normal pressure and near liquid nitrogen temperature as well as that of gaseous hydrogen at room temperature and pressure of ∼5 bar. The comparison of these spectra showed that hydrogenation strongly affected the phonon spectrum of the lithium silicate glass as was observed earlier for hydrogenated pure silica glass.[23] Both spectra contain wide bands at 4100−4200 cm^{-1} that obviously should be attributed to the stretching vibrational mode of a hydrogen molecule. The shape of the low-frequency region 100−800 cm^{-1} is also similar to that observed earlier for the hydrogenated pure silica glass SiO_2−H_2 and contains wide bands of the lithium silicate glass matrix and rather narrow bands of H_2 rotational modes near 319 (para-hydrogen) and 552 (ortho-hydrogen) cm^{-1}.[35]

However, the spectrum of hydrogenated lithium silicate glass LS6 is distinct from that of SiO_2−H_2. The stretching vibration band of H_2 in the spectrum of hydrogenated lithium silicate

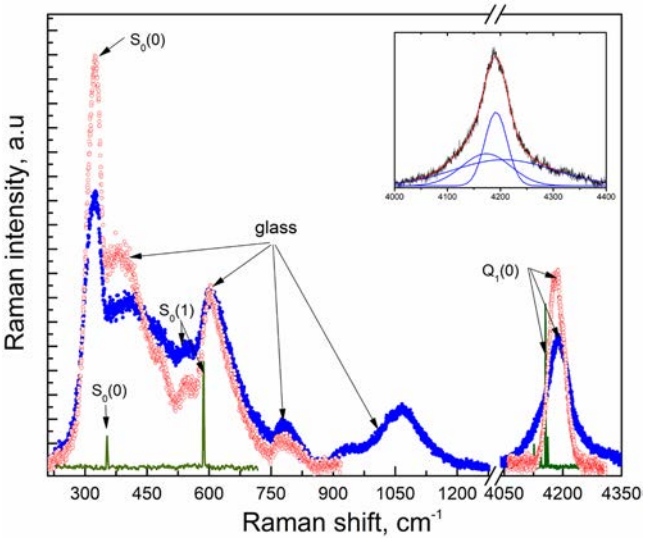

Figure 2. Raman spectra of the 0.6H_2−SiO_2 (open red circles)[24] and $Li_2O{\cdot}6SiO_2$-0.39H_2 (solid blue circles) samples at ambient pressure and $T \approx$ 85 K. Solid line: the Raman spectrum of gaseous hydrogen at room temperature and 0.5 MPa.[35] Inset: decomposition of the vibrational band in the Raman spectrum of the $Li_2O{\cdot}6SiO_2$-0.39H_2 sample into individual bands.

glass LS6 is wider than that in the spectrum of SiO_2−H_2. The deconvolution of this band (upper inset in Figure 2) showed that it contained three Gaussian bands with different bandwidths at frequencies of 4173, 4191, and 4206 cm^{-1}. The first and last bands were broader than the central band at 4191, which led to the total broadening of the H_2 stretching vibration band in LS6−0.39H_2 as compared to that in SiO_2−H_2. The frequencies of all components were higher than those of gaseous hydrogen, which could denote a shorter H−H bond length in the H_2 molecule dissolved in LS6 and the pure silica glass.

No stretching vibration bands of Si−H, Si−OH, or Li−OH were observed in the corresponding frequency regions of the measured Raman spectra. This suggests that, if other species are present in the quenched samples, their concentration is extremely low enough to be detected by the spectroscopic technique used. Considering this, we suggest that hydrogen gas released during hot extraction is due to the breaking of the van der Waals interaction between the dissolved H_2 molecule and the lithium silicate network.

The release of hydrogen during hot extraction in the pre-evacuated volume or under isothermal heating in the Raman experiments has a thermal activation character. The temperature region of hydrogen desorption of the hydrogenated samples depends on the values of energy of the interaction between a hydrogen molecule and the environment. The energy of this interaction is related to the value of the activation energy of hydrogen desorption in the hydrogenated samples. The activation energy can be determined from the measurements of the time dependences of the hydrogen content in the compound under isothermal heating at different temperatures. The time constant τ of the exponential decay obtained from these curves depends on temperature according to the Arrhenius formula:

$$\tau(T) = A{\cdot}\exp(E_A/k_BT) \quad (1)$$

https://doi.org/10.1021/acs.jpcc.3c02644
J. Phys. Chem. C 2023, 127, 13538−13546

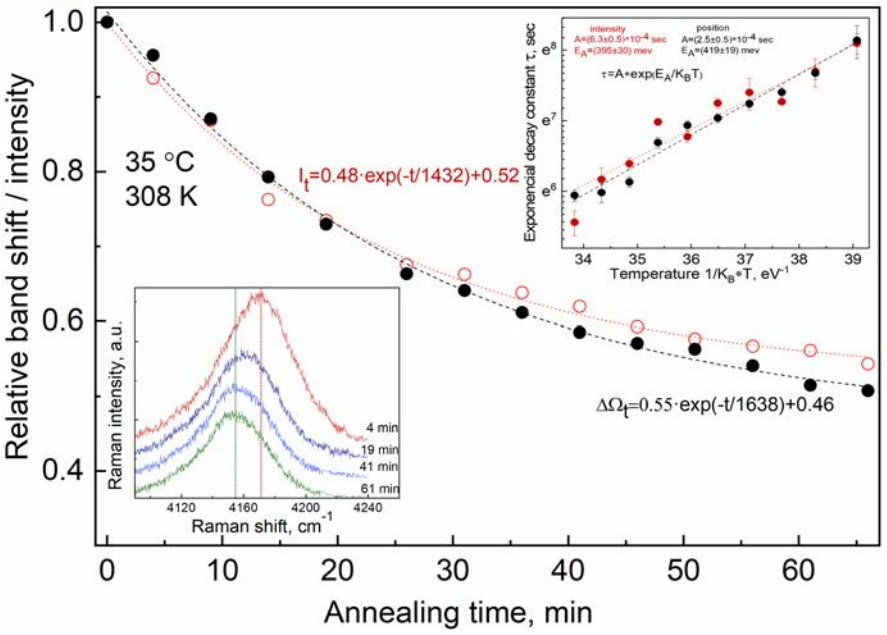

Figure 3. Relative shift (filled circles) and intensity (empty circles) of the vibration hydrogen mode in the $Li_2O{\cdot}6SiO_2$-$0.39H_2$ sample at 308 K as a function of the annealing time. Dashed lines: approximation by the exponential decay functions. Bottom inset: Raman spectra of the hydrogenated lithium silicate glass in the energy region of 3900−4260 cm^{-1} during annealing at 303 K after 4, 19, 41, and 61 min. Upper inset: Arrhenius plot of the exponential decay time constants τ obtained from the relative band shift (black circles) and intensity (red circles) as functions of the reciprocal annealing temperature $1/k_BT$ and their linear approximations (dotted lines). E_A is the activation energy, A is the time constant, and k_B is the Boltzmann constant.

where E_A is the activation energy, A is the time constant, and k_B is the Boltzmann constant.

Recently we have studied the desorption kinetics of the hydrogenated pure silica glass and SiO_2 opal matrices by Raman spectroscopy.[24,36] The kinetics of hydrogen desorption was studied *in situ* by tracking changes in the intensities of the para-hydrogen rotational modes upon heating. The data collected at different annealing temperatures gave activation energy of desorption E_a = 0.16 ± 0.01 eV/H_2 for both compounds.

The use of this method to determine the activation energy of the decomposition of a hydrogen solution in lithium silicate glass is rather difficult. This is related to the range of temperatures at which the emission of hydrogen begins (T = 0−100 °C), and the intensity of the rotational mode of para-hydrogen significantly decreases because of the hydrogen ortho-para conversion. In contrast to the previously used para-hydrogen mode, the ortho-rotational mode strongly overlaps with the lithium silicate glass modes; thus, the estimation of its relative intensity has a significant error. In the previous work,[36] we measured the intensity of the stretching vibrational mode of a hydrogen molecule as a function of the annealing time. As in the case of the para-rotational mode, the obtained dependence decreased according to an exponential law, which also indicated the relationship between the intensity of the vibrational mode and the hydrogen content as well as the activation character of the decomposition of this hydrogen solution.

The lower inset in Figure 3 shows the vibrational modes of hydrogen in the lithium silicate glass LS6 taken at T = 35 °C at various exposure times. As can be seen from the figure, with an increase in the annealing time, the intensity of the band decreases and also shifts to lower frequencies. The obtained intensity values and positions of the stretching vibration band depending on the annealing time are marked with open and filled circles in the main part of Figure 3.

The intensity values are well-fitted by the exponential decay function $I_{H2} = A{\cdot}\exp(-t/\tau) + B$. Note that the dependence of the Raman shifts of the H_2 vibrational mode is also well-approximated by the same function with almost coincident values of parameters A, B, and τ, which allows using the shift of the band to determine the decay time constant independently. The data obtained for the $Li_2O{\cdot}6SiO_2$-$0.39H_2$ samples annealed at various temperatures in the range of 21−70 °C and different exposure times show the exponential dependence of hydrogen desorption on time with the time constant varying from τ = 381 s at T = 70 °C to τ = 3482 s at T = 21 °C. The exponential dependence of hydrogen content on the annealing time and a decrease in the time constant of the exponential decay with an increasing annealing temperature indicate the activation character of hydrogen desorption in the $Li_2O{\cdot}6SiO_2$-$0.39H_2$ sample. The upper inset in Figure 3 shows the obtained values of τ in the Arrhenius coordinates and their approximation by the Arrhenius dependence (1). The activation energy values obtained from the intensities (red circles) and positions (black circles) of the stretching vibration peak almost coincide within the experimental error and are E_A = (0.395 ± 0.03) eV and E_A = (0.419 ± 0.019) eV, respectively. The pre-exponential constants A = (6.3 ± 0.5)$.10^{-4}$ s and A = (2.5 ± 0.5)$.10^{-4}$ s are also close to each other.

By using the change in the Raman shift of the stretching vibrational band of a hydrogen molecule with the annealing time, we also studied the decomposition of solid solutions of similar compositions $Li_2O{\cdot}6SiO_2$-0.22/0.25H_2. The obtained dependencies of the Raman shift of the stretching vibrational band on the annealing time due to a change in the hydrogen content also had an exponential decay character. Figure 4

https://doi.org/10.1021/acs.jpcc.3c02644
J. Phys. Chem. C 2023, 127, 13538−13546

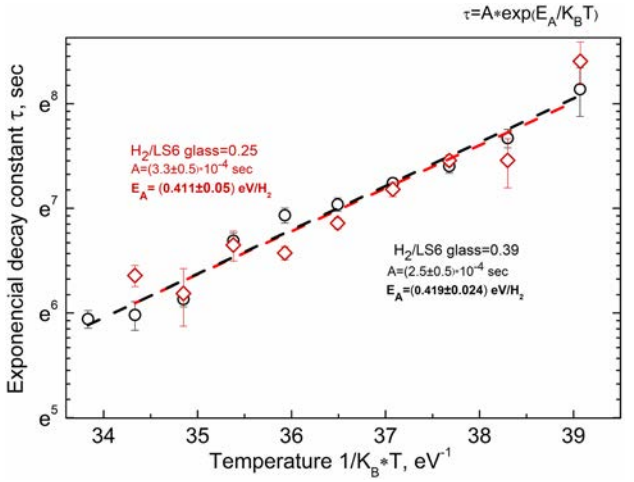

Figure 4. Arrhenius plot $\tau(T) = A{\cdot}\exp(E_A/k_BT)$ of the dependence of the exponential decay time constant τ on the annealing temperature $1/k_BT$ (open symbols) and its linear approximation (dotted line). Open diamonds and open circles relate to the decomposition of $Li_2O{\cdot}6SiO_2$-$0.25H_2$ and $Li_2O{\cdot}6SiO_2$-$0.39H_2$, respectively.

demonstrates the obtained time constants τ in the Arrhenius coordinates for $Li_2O{\cdot}6SiO_2$-$0.22/0.25H_2$ compared to the time constants for the $Li_2O{\cdot}6SiO_2$-$0.39H_2$ solution. The fitting of the obtained τ values for the $Li_2O{\cdot}6SiO_2$-$0.22/0.25H_2$ solutions by the Arrhenius dependence gives the activation energy E_A = (0.411 ± 0.06) eV with the pre-exponential A = $3.3{\cdot}10^{-4}$ s. These values of the activation energy and the pre-exponential constant are very close to the values E_A = (0.419 ± 0.019) eV and A = $2.5{\cdot}10^{-4}$ obtained for the $Li_2O{\cdot}6SiO_2$-$0.39H_2$ solution. Thus, the decomposition of solid solutions of hydrogen in the LS6 glass has a thermal activation type of behavior with almost the same Arrhenius dependence parameters regardless of the initial content of dissolved hydrogen.

Besides the Raman spectroscopy data, the hydrogen desorption kinetics was also studied by tracking changes in the pressure of hydrogen gas released in the pre-evacuated vessel during the isothermal heating of the hydrogenated LS6 samples. The measured pressure was recalculated in terms of the amount of released gas subtracted from the initial content for every time point at a constant temperature. Figure 5 demonstrates some time dependencies of H_2 relative content $C(t) = X_t/X_0$ obtained in the temperature range of 0−90 °C for the LS6−$0.39H_2$ sample, where X_0 is the initial hydrogen content and X_t is the hydrogen content at the current time t. Each plotted curve can be adequately fitted by the sum of two exponential decay functions $C(t) = C_1{\cdot}\exp(-t/\tau_1) + C_2{\cdot}\exp(-t/\tau_2)$ with an R^2 of not less than 0.99. The parameters of these functions for isothermal desorption procedures at several temperatures are given in Table 1.

The C_1 and C_2 parameters are related to the parts of hydrogen that participate in the corresponding decay process. The main difference between these decay functions is the value of the time constants τ_1 and τ_2, which differ by ∼20−60 times. Thereby, both the weights and time constants of decay functions $C(t)$ indicate that the decomposition of H_2 solutions in the lithium silicate glass LS6 can be divided into two parallel decay processes with "fast" and "slow" rates. Figure 6 shows all of these τ constants for the LS6−$0.25/0.22H_2$ and LS6−$0.39H_2$ samples plotted in the Arrhenius coordinates.

The approximation of these data by Arrhenius dependencies allowed us to obtain four activation energies and pre-exponential constants for the "slow-rate" and "fast-rate" processes of the LS6−$0.25/0.22H_2$ and LS6−$0.39H_2$ sample decay. The desorption reaction of the LS6−$0.25/0.22H_2$ sample had the measured activation energy E_A of (0.161 ± 0.043) eV/H_2 molecule and the constant A = 33.11 s for the "slow-rate" decay and (0.128 ± 0.024) eV/H_2 molecule; A = 2.09 s for the "fast-rate" one. The activation energies of the LS6−$0.39H_2$ decay had close values of E_A = (0.206 ± 0.03) and (0.195 ± 0.015) eV/H_2 molecule for the "slow-rate" and fast-rate decays, respectively; while the pre-exponential constants for this sample differed in magnitude by more than 25 times (A = 4.66 and 0.18 s, respectively).

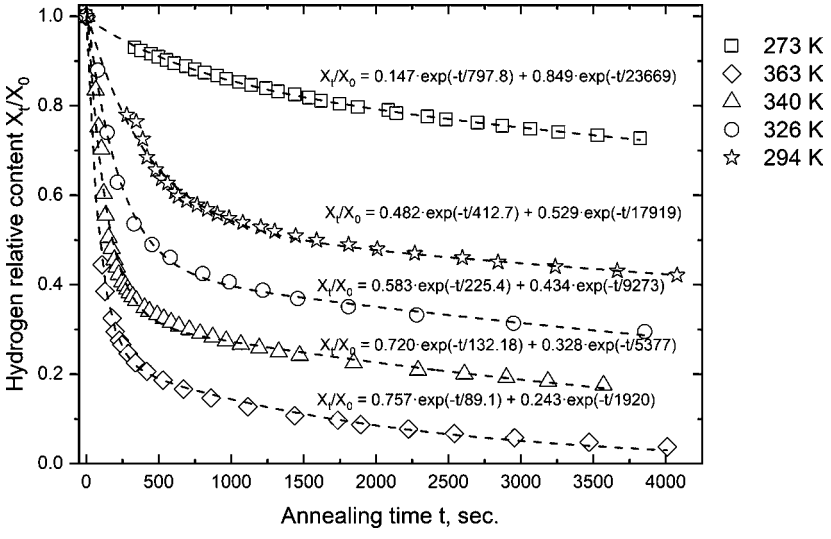

Figure 5. Time dependence of the relative hydrogen content C_t/C_0 of $Li_2O{\cdot}6SiO_2$-$0.39H_2$ under annealing at 273, 294, 326, 340, and 363 K (open symbols) obtained by tracking changes in the pressure in the pre-evacuated system; dashed lines: fitting of the experimental data by the exponential decay functions.

https://doi.org/10.1021/acs.jpcc.3c02644
J. Phys. Chem. C 2023, 127, 13538−13546

Table 1. Parameters of the Decay Functions Used to Approximate the LS6-0.25H_2 and LS6-0.39H_2 Decomposition Data Obtained from the Pressure Increase in the Pre-Evacuated System at Different Temperatures

		LS6−0.39H_2		
T, K	τ_1, sec	C_1	τ_2, sec	C_2
273 ± 1	797.8	0.14711	23669	0.84915
	±47.3	±0.00624	±1303	±0.0068
293 ± 0.567	412.7	0.4822	17920	0.52919
	±24.1	±0.0159	±3195	±0.01397
311 ± 0.356	240.7	0.47324	9523	0.55614
	±11.5	±0.01013	±762	±0.00897
326 ± 0.397	225.5	0.58357	9274	0.43491
	±17.1	±0.02049	±1677	±0.01717
333 ± 0.25	137.60	0.54428	7460	0.46107
	±5.3	±0.01145	±552	±0.00766
340 ± 0.35	132.2	0.72002	5377	0.3282
	±7.5	±0.02282	±805	±0.01329
360 ± 0.415	125.8	0.71028	4299	0.29035
	±2.9	±0.0095	±208	±0.00514
363 ± 1.16	89.1	0.75718	1920	0.24261
	±2.1	±0.0092	±87	±0.0062
LS6−0.25H_2				
305.4 ± 0.267	295.97	0.361	15705	0.647
	±16.69	±0.01	±1352	±0.008
323.46 ± 0.594	196.9	0.40769	12779	0.60583
	±12.2	±0.01162	±1190	±0.00908
335 ± 0.30	148.5	0.50091	7329	0.49968
	±6.4	±0.01194	±592	±0.00905
346 ± 0.109	153.5	0.44346	6014	0.55433
	±5.5	±0.00812	±195	±0.00554
370.33 ± 0.747	124.6	0.63302	6157	0.41468
	±14.2	±0.03595	±1559	±0.0267

DISCUSSION

Among all systems containing molecular hydrogen, the SiO_2-XH_2 solid solutions have Raman spectra that are most similar to those of LS6-XH_2 under study. This fact can indicate the similarity of both the network structure and the hydrogen molecule states in these solid solutions. Thus, it would be wise to compare the decompositions of the LS6-XH_2 and SiO_2-XH_2 solid solutions. According to the data obtained by Raman spectroscopy in this work, the decay of LS6−0.39H_2 and LS6−0.25/0.22H_2 occurred with the activation energy E_A = (0.419 ± 0.019) eV and E_A = (0.411 ± 0.06) eV, respectively. These values much exceed the activation energy E_A = (0.16 ± 0.02) eV that was observed earlier for the decay of SiO_2-0.7H_2,[24] and this means a considerably stronger interaction between the hydrogen molecules and the lithium silicate network than van der Waals forces. As the activation energies of the LS6-XH_2 decay are in the range of energy values of 0.1−0.8 eV/H_2 characteristic of the Kubas interaction, we assume that these large values of activation energies can be due to the Kubas forces arising from the interaction between the hydrogen molecules and the lithium cations.

The data on the decay process of LS6-XH_2 obtained by the hot desorption method differ significantly from those obtained by Raman spectroscopy. First, the values of the activation energies obtained from these data are two to three times lower than the activation energy of the decay process obtained by Raman spectroscopy wherein the pre-exponential constants are higher by several orders of magnitude. We assume that this difference in the activation energies and pre-exponential constants obtained by the two methods is due to the difference in the research approaches used for the study of the decay processes. Raman backscattering spectroscopy studies a change in the hydrogen concentration that occurs within the laser beam spot with a diameter of several micrometers on the sample surface. In this case, the decay activation energy may be associated mainly with hydrogen desorption from the sample surface and can be attributed to the surface barrier that must be overcome for a hydrogen molecule to escape from the sample. When studying the desorption processes by the hot extraction method, we determined a change in the hydrogen concentration in the entire sample with characteristic dimensions of several millimeters. To escape from a lithium-silicate glass sample, hydrogen molecules must not only break away from the surface by overcoming the barrier in the near-surface layer but also pass through the entire volume of the sample before that. In this case, hydrogen diffusion has a great

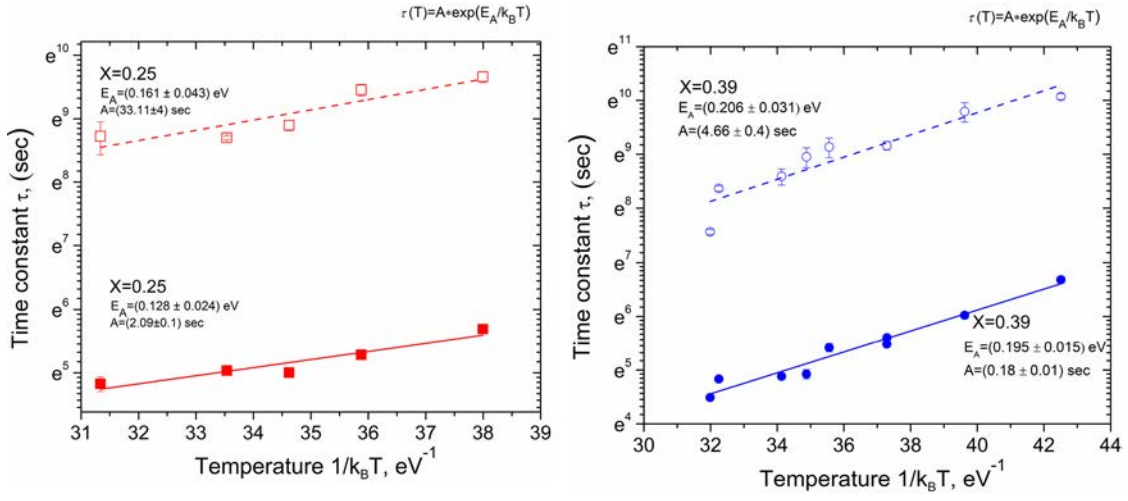

Figure 6. Time constants τ for decomposition of the $Li_2O{\cdot}6SiO_2$-0.39H_2 (full and open circles, right panel) and $Li_2O{\cdot}6SiO_2$-0.25H_2 (full and open squares, left panel) solutions annealed at different temperatures *T* in the pre-evacuated system. The dashed and solid lines are linear fits to the experimental data for two parallel activation processes.

https://doi.org/10.1021/acs.jpcc.3c02644
J. Phys. Chem. C 2023, 127, 13538−13546

impact on the desorption time. Then, the activation energy and time constants of solution decomposition determined by the hot desorption method are some effective quantities into which the processes of hydrogen diffusion in the sample and its subsequent escape from the surface are summed up. The second peculiarity of the data obtained by hot desorption method is that the decay of both LS6-0.39H_2 and LS6-0.25/0.22H_2 is characterized by the existence of two parallel decay processes with time constants differing by 20−60 times at various temperatures. It is known that under cooling the $Li_2O{\cdot}_6SiO_2$, melt should decompose into regions enriched and depleted with lithium cations.[37] In this case, glass obtained from a melt of this composition should also contain such regions. Obviously, both the processes of diffusion of hydrogen in such regions and its escape from their surface must differ from each other. According to the data on helium diffusion in the lithium silicate glass,[38] it can be assumed that the release of hydrogen from regions containing less than 10 mol % lithium oxide should be similar to the process of decomposition of hydrogenated pure silica glass. Recall that the activation energy of hydrogen desorption in the near-surface region of hydrogenated pure silica glass is EA = 0.16 eV/H_2 molecule, and the activation energy of diffusion of the H_2 molecule in pure silica glass is ED = 0.52 eV/H_2 molecule.[39] The "fast-rate" process of LS6-0.39H_2 and LS6-0.25/0.22H_2 decomposition detected by hot desorption may correspond to hydrogen release from lithium-depleted regions. At the same time, the release of hydrogen from lithium-enriched regions should occur with higher activation energies of diffusion and decay. In this regard, the value of the activation energy of decay from the surface layer EA = (0.419 ± 0.019) eV determined by Raman spectroscopy may refer to hydrogen release from lithium-enriched regions. Note that the data in Raman experiments are usually obtained 5−7 min after the sample was placed on the microscope stage, i.e., after the end of the "fast-rate" decay process. As regards, the activation energy of diffusion of the H_2 molecule through lithium-enriched regions, we can only assume that its value should be higher than 0.52 eV/H_2 determined for pure silica glass.[39] This assumption is supported by the previously determined increase in the activation energy of helium diffusion with an increase in the lithium content.[38]

The value of the surface activation barrier E_A = (0.419 ± 0.019) eV and the assumed value of the diffusion barrier E_D > 0.52 eV/H_2 are higher than the "total" decay activation energy of E_A = (0.206 ± 0.03) obtained by hot desorption. This phenomenon may occur if the characteristic values of time constants for diffusion processes significantly exceed the values of time constants for surface processes. In this case, the time constants determined by the hot desorption method should lie between these two dependencies in the Arrhenius coordinates.

According to the data of ref 24, the characteristic time of the decomposition of the hydrogenated pure silica glass is $\tau \approx 13$ s at the decay activation energy E_A = 0.16 eV/H_2, the constant A = 0.027 s, and the temperature T = 25 °C. The data obtained by Raman spectroscopy in this work show that the time constant of the decomposition of a hydrogen solution in the lithium silicate glass at room temperature is τ = 3220 s. The time constant increases by 3 orders of magnitude as compared to silica glass due to an increase in the decay activation energy by 2.6 times to E_A = 0.42 eV/H_2 molecule despite a decrease in the constant A by 2 orders of magnitude. In addition, according to the hot desorption data, the time constants of hydrogen escape from the lithium silicate glass at room temperature are 1 order of magnitude higher than this value. This fact also points to the existence of an additional activation barrier inside the bulk lithium silicate glass, which may be due to the peculiarities of the hydrogen diffusion in it.

CONCLUSIONS

The hydrogen solutions in the bulk lithium silicate glass $Li_2O{\cdot}6SiO_2$ (LS6) were synthesized for the first time at pressures of 6.7−7.5 GPa and a temperature of 280 °C. The study of the composition by thermal desorption with continuous heating showed that 1 mol of the glass contained 0.25 and 0.39 mol of hydrogen, most of which was released in the pre-evacuated volume above room temperature. A similar study of hydrogen desorption from silica glass showed that the same amount of hydrogen was released from it at temperatures significantly below room one.[24] The Raman study carried out at liquid nitrogen temperature and normal pressure demonstrated that, in addition to the lines of the glass itself, the spectra of both solutions in the lithium silicate glass also contained the lines at frequencies of about 319, 552, and 4155−4219 cm^{-1} that corresponded to the rotational and vibrational modes of molecular hydrogen. At the same time, no lines were found corresponding to strong bonds of hydrogen with the lattice, such as Li−H, Si−H, or Si−OH. To understand the reason for the thermal stability of this solution of molecular hydrogen relative to a solution of hydrogen in pure silica glass, the kinetics of its desorption was studied by Raman spectroscopy and hot desorption in the pre-evacuated volume in the temperature range of 0−97 °C. The study of the time-dependent shift and a decrease in the intensity of the hydrogen stretching vibration band under annealing at various temperatures showed that the activation energies of desorption from the sample surface were E_A = (0.419 ± 0.019) eV and E_A = (0.411 ± 0.06) eV for the LS6−0.39H_2 and LS6−0.25/0.22 H_2 solutions, respectively. Taking into account such a high value of the activation energy of the decomposition of the solution, which is not characteristic of the van der Waals interaction, we assume that its high thermal stability is due to the emergence of the "Kubas" interaction between hydrogen molecules and the silicate network initiated by the lithium cations. This interaction leads to an increase in the time constant τ of the decomposition of a hydrogen solid solution in the lithium silicate glass at room temperature by several thousand times to τ = 3220 s as compared to the decomposition of a hydrogen solution in pure silica glass (τ = 3 s). The results obtained by hot desorption during isothermal annealing in a pre-evacuated vessel showed that the activation energy of hydrogen diffusion that might be higher than 0.51 eV also had a great impact on the stability of a hydrogen solution in the bulk lithium silicate glass, which additionally increased the decay time constant to $\tau \approx$ 16 000 s at room temperature.

AUTHOR INFORMATION

Corresponding Author

V. S. Efimchenko − *Institute of Solid State Physics, Russian Academy of Sciences, Chernogolovka 142432 Moscow Region, Russia;* orcid.org/0000-0002-4791-1499;
Email: efimchen@issp.ac.ru

https://doi.org/10.1021/acs.jpcc.3c02644
J. Phys. Chem. C 2023, 127, 13538−13546

Authors

M. A. Korotkova − *Institute of Solid State Physics, Russian Academy of Sciences, Chernogolovka 142432 Moscow Region, Russia*

K. P. Meletov − *Institute of Solid State Physics, Russian Academy of Sciences, Chernogolovka 142432 Moscow Region, Russia*

S. Buchner − *Institute of Physics, Federal University of Rio Grande do Sul (UFRGS), Porto Alegre 9150-970, Brazil*

Complete contact information is available at: https://pubs.acs.org/10.1021/acs.jpcc.3c02644

Notes

The authors declare no competing financial interest.

■ ACKNOWLEDGMENTS

The study was supported by the Russian Science Foundation grant No. 23-23-00426, https://rscf.ru/en/project/23-23-00426/.

■ REFERENCES

(1) García-holley, P.; Schweitzer, B.; Islamoglu, T.; et al. Benchmark study of hydrogen storage in metal-organic frameworks under temperature and pressure swing conditions. *ACS Energy Lett.* **2018**, *3*, 748−754.

(2) Liu, H.; Wang, X.; Liu, Y.; Dong, Z.; Ge, H.; Li, S.; Yan, M. Hydrogen desorption properties of the MgH_2−AlH_3 composites. *J. Phys. Chem. C* **2014**, *118*, 37−45.

(3) Terent'ev, P. B.; Gerasimov, E. G.; Mushnikov, N. V.; et al. Kinetics of hydrogen desorption from MgH_2 and AlH_3 hydrides. *Phys. Metals Metallogr.* **2015**, *116*, 1197−1202.

(4) Zhang, J.; Li, Z.; Wu, Y.; et al. Recent advances on the thermal destabilization of Mg-based hydrogen storage materials. *RSC Adv.* **2019**, *9*, 408−428.

(5) Luo, Q.; Li, J.; Li, B.; Liu, B.; Shao, H.; Li, Q. Kinetics in Mg-based hydrogen storage materials: enhancement and mechanism. *J. Magnes. Alloy* **2019**, *7*, 58−71.

(6) Dalebrook, A. F.; Gan, W.; Grasemann, M.; Moret, S.; Laurenczy, G. Hydrogen storage: beyond conventional methods. *Chem. Commun. (Camb)* **2013**, *49*, 8735−8751.

(7) Chen, Z.; Kirlikovali, K. O.; Idrees, K. B.; Wasson, M. C.; Farha, O. K. Porous materials for hydrogen storage. *Chem.* **2022**, *8*, 693−716.

(8) Li, Y.; Xiao, Y.; Dong, H.; Zheng, M.; Liu, Y. Polyacrylonitrile-based highly porous carbon materials for exceptional hydrogen storage. *Int. J. Hydrogen Energy* **2019**, *44*, 23210−23215.

(9) Germain, J.; Fréchet, J. M.; Svec, F. Nanoporous polymers for hydrogen storage. *Small* **2009**, *5*, 1098−1111.

(10) Sun, G.; Tangpanitanon, J.; Shen, H.; et al. Physisorption of molecular hydrogen on carbon nanotube with vacant defects. *J. Chem. Phys.* **2014**, *140*, 204712−204716.

(11) Panchariya, D. K.; Rai, R. K.; Anil Kumar, E.; Singh, S. K. Core-shell zeolitic imidazolate frameworks for enhanced hydrogen storage. *ACS Omega* **2018**, *3*, 167−175.

(12) Lee, S.; Lee, J.; Kim, Y.; Kim, J.; Lee, K.; Park, S. Recent progress using solid-state materials for hydrogen storage: a short review. *Processes* **2022**, *10*, 304−322.

(13) Kubas, G. J.; Ryan, R. R.; Swanson, B. I.; Vergamini, P. J.; Wasserman, H. J. Characterization of the first examples of isolable molecular hydrogen complexes, M(CO)3 (PR3) 2 (H2) (M = molybdenum or tungsten; R = Cy or isopropyl). Evidence for a side-on bonded dihydrogen ligand. *J. Am. Chem. Soc.* **1984**, *106*, 451−452.

(14) Vitillo, J. G.; Regli, L.; Chavan, S.; et al. Role of exposed metal sites in hydrogen storage in MOFs. *J. Am. Chem. Soc.* **2008**, *130*, 8386−8396.

(15) Zhou, W.; Yildirim, T. Nature and tunability of enhanced hydrogen binding in metal-organic frameworks with exposed transition metal sites. *J. Phys. Chem. C* **2008**, *112*, 8132−8135.

(16) Niu, J.; Rao, B. K.; Jena, P. Binding of hydrogen molecules by a transition-metal ion. *Phys. Rev. Lett.* **1992**, *68*, 2277−2281.

(17) Liu, Y.; Su, B.; Dong, W.; Li, Z. H.; Wang, H. Structural characterization of a boron(III) η 2 -σ-silane-complex. *J. Am. Chem. Soc.* **2019**, *141*, 8358−8363.

(18) Bhattacharya, S.; Bhattacharya, A.; Das, G. P. Anti-Kubas type interaction in hydrogen storage on a Li decorated BHNH sheet: a first-principles based study. *J. Phys. Chem. C* **2012**, *116*, 3840−3844.

(19) Chung, C.; Ihm, J.; Lee, H. Recent progress on Kubas-type hydrogen-storage nanomaterials: from theories to experiments. *J. Korean Phys. Soc.* **2015**, *66*, 1649−55.

(20) Lang, C.; Jia, Y.; Yan, X.; Ouyang, L.; Zhu, M.; Yao, X. Molecular chemisorption: a new conceptual paradigm for hydrogen storage. *Chem. Synth.* **2022**, *2*, 1−13.

(21) Efimchenko, V. S.; Fedotov, V. K.; Kuzovnikov, M. A.; Zhuravlev, A. S.; Bulychev, B. M. Hydrogen solubility in amorphous silica at pressures up to 75 kbar. *J. Phys. Chem. B* **2013**, *117*, 422−425.

(22) Efimchenko, V. S.; Barkovskii, N. V.; Fedotov, V. K.; et al. High-pressure solid solutions of molecular hydrogen in amorphous magnesium silicates. *J. Alloys Comp.* **2019**, *770*, 229−235.

(23) Meletov, K. P.; Efimchenko, V. S. Raman study of hydrogen-saturated silica glass. *Int. J. Hydrogen Energy* **2021**, *46*, 24501−24509.

(24) Meletov, K. P.; Efimchenko, V. S. Stability of hydrogenated silica glass and desorption kinetics of molecular hydrogen. *Chem. Phys. Lett.* **2022**, *793*, 139477−139480.

(25) Abdeyazdan, H.; Shevchenko, M.; Hayes, P. C.; et al.. Integrated experimental and thermodynamic modeling investigation of phase equilibria in the PbO−MgO−SiO_2 System in air. *Metall. Mater. Trans. B* **2022**, *53*, 954−967.

(26) Tangeman, J. A.; Phillips, B. L.; Navrotsky, A.; et al. Vitreous forsterite (Mg_2SiO_4): Synthesis, structure, and thermochemistry. *Geophys. Res. Lett.* **2001**, *28*, 2517−2520.

(27) Efimchenko, V. S.; Barkovskii, N. V.; Fedotov, V. K.; Meletov, K. P.; Chernyak, V. M.; Khryapin, K. I. Destruction of fayalite and formation of iron and iron hydride at high hydrogen pressures. *Phys. Chem. Minerals* **2019**, *46*, 743−749.

(28) Efimchenko, V. S.; Barkovskii, N. V.; Fedotov, V. K.; Meletov, K. P.; Prokoshin, A. V. Chemical reactions in the Fe_2SiO_4-D_2 system with a variable deuterium content at 7.5 GPa. *Am. Mineral.* **2021**, *106*, 1097−1104.

(29) Konar, B.; Van Ende, M. A.; Jung, I. H. Critical evaluation and thermodynamic optimization of the Li-O, and Li_2O-SiO_2 systems. *J. Europ. Ceram. Soc.* **2017**, *37*, 2189−2207.

(30) Lee, S-Ch.; Hur, J.-M.; Seo, Ch-S. Silicon powder production by electrochemical reduction of SiO_2 in molten LiCl−Li_2O. *J. Indust. and Eng. Chem.* **2008**, *14*, 651−654.

(31) Khvostantsev, L. G.; Slesarev, V. N.; Brazhkin, V. V. Toroid type high-pressure device: history and prospects. *High Pres. Res.* **2004**, *24*, 371−383.

(32) Antonov, V. E.; Bulychev, B. M.; Fedotov, V. K.; Kapustin, D. I.; Kulakov, V. I.; Sholin, I. A. NH_3BH_3 as an internal hydrogen source for high pressure experiments. *Int. J. Hydrogen Energy* **2017**, *42*, 22454−22459.

(33) Bashkin, I. O.; Antonov, V. E.; Bazhenov, A. V.; Bdikin, I. A.; Borisenko, D. N.; et al. Thermally stable hydrogen compounds obtained under high pressure on the basis of carbon nanotubes and nanofibers. *JETP Lett.* **2004**, *79*, 226−230.

(34) Meletov, K. P. A nitrogen cryostat with adjustable temperature and cold loading of samples for the measurement of optical spectra. *Instrum. Exp. Technol.* **2020**, *63*, 291−293.

(35) McLennan, J. C.; McLeod, J. H. The Raman effect with liquid oxygen, nitrogen, and hydrogen. *Nature* **1929**, *123*, 160.

(36) Meletov, K. P.; Efimchenko, V. S.; Korotkova, M. A.; Masalov, V. M.; Sukhinina, N. S.; Emel'chenko, G. A. Peculiarities of the absorption and desorption of hydrogen by opal matrices. *Int. J. Hydrogen Energy* **2023**, *48*, 14337−14347.

(37) Haller, W.; Blackburn, D. H.; Simmons, J. H. Miscibility gaps in alkali-silicate binaries—data and thermodynamic interpretation. *J. Am. Ceram. Soc.* **1974**, *57*, 120−126.
(38) Shelby, J. E. Helium migration in lithium aluminosilicate glasses. *J. of Appl. Phys.* **1977**, *48*, 1497−1502.
(39) Shang, L.; Chou, I.-M.; Lu, W.; Burruss, R. C.; Zhang, Y. Determination of diffusion coefficients of hydrogen in fused silica between 296 and 523 K by Raman spectroscopy and application of fused silica capillaries in studying redox reactions. *Geoch. et Cosm. Acta.* **2009**, *73*, 5435−5443.

https://doi.org/10.1021/acs.jpcc.3c02644
J. Phys. Chem. C 2023, 127, 13538−13546